# Tunable Contact Conditions and Grasp Hydrodynamics Using Gentle Fingertip Suction

Hannah S. Stuart, *Member, IEEE*, Shiquan Wang, and Mark R. Cutkosky, *Fellow, IEEE*

***Abstract*—Gentle suction flow at the fingertips of a compliant hand can enhance object acquisition and increase the robustness of pinch grasps under water. The approach adds a low-pressure pump and flexible tubes that terminate at the distal phalanges. The light flow rate does not create a powerful suction force, nor does it stir up significant sediment. The method works on porous and rough objects in addition to smooth objects as it does not require forming a seal. It changes contact conditions—normal force and coefficient of friction—and enlarges the acquisition region when grasping free objects under water. A simple hydrodynamic model matches empirical force measurements adequately for incorporation in a dynamic simulation to explore the effects of flow rate and object mass. Simulations and experiments show that effects of fingertip suction flow are most pronounced for acquiring objects on the order of 1 kg or less and when pinching large objects. Gentle suction flow is an effective, versatile, and convenient addition for robots that must grasp and manipulate objects under water.**

***Index Terms*—Contact modeling, dynamics, grasping, marine robotics, multifingered hands.**

## I. Introduction

REMOTE robotic manipulation is an important tool for ocean exploration. Underwater vehicles can take the place of divers, especially at dangerous depths, and expand our access to untapped marine environments. Applications range from oil rig maintenance to ocean archeology and marine biology. However, the underwater environment also presents formidable challenges for robotic manipulation: slippery biofilms are commonplace, water currents can make reaching for flexible objects inaccurate, and buoyancy can make it easy to accidentally push floating objects away while trying to grasp them. Improved dexterity and grasp reliability could allow robotic diving platforms to function more effectively.

This work is an extension of the Red Sea Robotics Exploratorium (RSRX), a collaboration between Stanford University and the King Abdullah University of Science and Technology (KAUST) to create a teleoperated humanoid diver.[1] For an overview of other underwater manipulation platforms, see the *Springer Handbook of Robotics* chapter by Antonelli *et al.* [2] and recent article by Zhang *et al.* [3]; notable projects include ALIVE [4], TRIDENT [5], and SAUVIM [6].

Suction flow is a common mechanism in aquatic animals. For example, many fish use suction feeding to capture prey [7]–[9]. In a similar way, suction flow at the fingertips of a robotic hand can enhance acquisition. Although biological mechanisms typically rely on short bursts of flow, we investigate a sustained flow provided by a small pump, which can be located at the base of an arm and connected via flexible tubing to orifices at the fingertips (see Fig. 1). Suction flow both attracts small objects to the fingertips and changes the friction conditions after making contact. Fig. 1 shows the RSRX hand picking up a bar of soap—a maneuver enabled here by fingertip suction flow.[2]

In this paper, we investigate two mechanisms by which gentle suction flow enhances underwater grasping and manipulation: hydrodynamic forces and contact reliability. We briefly describe the RSRX hand in Section II and present a simple hydrodynamic model of the suction flow forces in Section III. The model matches empirical results well enough for incorporation into a dynamic simulation to investigate the role of suction on grasping in Section IV. Suction flow also helps maintain a static pinch between the fingertips. Section V explores the effects of suction on pinch strength for objects of varying size, smoothness, and friction coefficient. Section VI demonstrates other potential roles of light fingertip flow.

This work builds on preliminary results in [10] and [11]. Suction force is characterized down to 200 $\mu$m of object–finger distance, and a simplified model is presented as a function of pump parameters. Dynamic simulations demonstrate the role of water drag, object mass, flow conditions, and hand–object alignment on the acquisition region. Results indicate that gentle suction flow is useful for grasping a wide range of objects

Manuscript received January 21, 2018; revised August 9, 2018; accepted October 2, 2018. Date of publication November 30, 2018; date of current version April 2, 2019. This paper was recommended for publication by Associate Editor R. Carloni and Editor P. Dupont upon evaluation of the reviewers' comments. This work was supported by the King Abdullah University of Science and Technology's Red Sea Robotic Exploratorium Stanford Agreement SPO 103760, and unrestricted laboratory funds. The work of H. S. Stuart was supported in part by the National Science Foundation Graduate Fellowship Program under Grant DGE-114747, in part by the Stanford Graduate Fellowship, and in part by the Gerald J. Lieberman Fellowship. *(Corresponding author: Hannah S. Stuart.)*

H. S. Stuart is with the Department of Mechanical Engineering, University of California, Berkeley, Berkeley, CA 94709 USA (e-mail: hstuart@berkeley.edu).

S. Wang is with Flexiv Robotics Ltd., Santa Clara, CA 95054 USA (e-mail: shiquan.wang@flexiv.com).

M. R. Cutkosky is with the Department of Mechanical Engineering, Stanford University, CA 94305 USA (e-mail: cutkosky@stanford.edu).

This paper has supplementary downloadable material available at http://ieeexplore.ieee.org, provided by the author. The material consists of a video, demonstrating four tasks: a bar of soap is picked up, a Lego block is pinched, a neutrally buoyant PVC tube is grasped, and a water balloon is transitioned into a wrap grasp. Contact hstuart@berkeley.edu for further questions about this work.

Color versions of one or more of the figures in this paper are available online at http://ieeexplore.ieee.org.

Digital Object Identifier 10.1109/TRO.2018.2880094

[1]The RSRX project was the first step in developing Ocean One [1] (see Fig. 1) and was intended for exploration of coral reefs in the Red Sea.

[2]An accompanying video submission demonstrates this task.

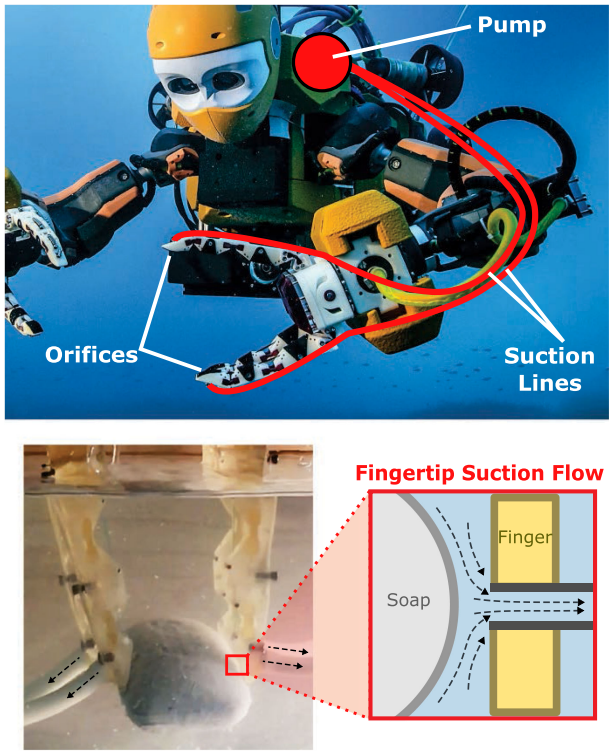


Fig. 1. (Top) Marine robots can benefit from distributed gentle suction flow through light attractive forces and an increase in the friction coefficient. Suction lines could run from a pump located at the base of the robot arm to the fingertips. (Bottom) With gentle suction flow at the fingertips, the RSRX hand is able to grasp and pinch a larger range of objects under water. Here, a slippery bar of soap is only acquired in a pinch when using suction flow.

and tools encountered or utilized in marine environments. An updated static pinch model is applied to investigate grasp security when resisting external object pullout forces, and a range of object surface properties is explored. Finally, reverse flow is introduced as a potential mechanism for in-hand manipulation. These studies provide deeper understanding as to the design of gentle suction flow for submerged end-effectors.

### A. *Suction for Manipulation*

Suction is a common astrictive solution [12] for robotic gripping. As noted in [13], eight of the 13 most successful groups in the first Amazon Picking Challenge utilized some form of suction, ranging from a single suction cup to combined suction-hand designs. For example, Team Delft won the competition relying heavily on an articulated high-flow suction cup [14]. Suction cups are susceptible to dropping an object if the cup seal is broken or the object is too heavy. For greater reliability, suction can be combined with a compliant gripper [15], leading to strategies like reorienting objects with a single suction point to better enclose them in a grasp. While most of the implementations are modular, with suction and grasping functionalities separated, Yamaguchi *et al.* [16] integrated suction orifices directly into the fingertips in an approach similar to that used for the RSRX hand presented here.

The foregoing solutions function in air. In water, the higher density and viscosity can increase suction efficacy. In particular, suction flow in water can affect objects at greater distances than in air and, on contact, can affect the tribology and friction. Unlike suction cups that require a seal, suction flow works on porous, rough, and even crumbling objects. Suction for gripping has been validated during ocean exploration, with a limpet-inspired venturi system utilized at deep sea archaeological sites [17], which uses continuous flow to ensure gripping even when a seal is not created.[3]

In this paper, we explore how fingertip suction improves multifinger handling under water. Overall, strength and security of compliant grasps are highly dependent upon contact conditions; suction flow affects those contact conditions directly for a disproportionate influence on the grasp.

### B. *Evaluation of Dynamic Underwater Grasping*

The role of hydrodynamics in robotic manipulation for arm- and vehicle-scale motions has been investigated for decades, as summarized in [2]. Less attention has been paid to finger motions, as fingers are slender so they are unlikely to produce substantial hydrodynamic effects. However, objects of a moderate size may incur significant drag forces during grasping maneuvers. This is important because quick grasping is a useful strategy when both the robot and the object are free-floating and subject to water currents and imperfect positioning that drifts over time.

A *grasp acquisition region* is the area around a hand in which objects will be pulled into a stable grasp; it is one way to characterize dynamic grasping capabilities. Previous works by Dollar and Howe [19], Kragten and Herder [20], and Aukes [21] explore one-, two-, and three-dimensional potential fields and quasi-static acquisition regions for underactuated hands. The larger the grasp region, the more forgiving the hand is to postural errors during robotic reaching and manipulation. This metric is utilized in Section IV.

Dynamic simulation is a particularly powerful tool for underwater hand evaluation, where friction and fluid drag affect grasping behavior. In this paper, we use SimGrasp [22], based on the Klamp't dynamics engine [23], for grasp simulations.

## II. Hand Design

Hands are extended from the body, so they disproportionately affect the inertia of the arm and are likely to collide with the world unintentionally. Underactuation is a useful way to reduce end-effector complexity and weight while improving resilience [24]. For these reasons, the RSRX hand is compliant and shares design elements with hands presented in [25]–[28]. Previous underactuated hands built for marine operation range from sensorized linkage driven mechanisms, such as SeeGrip [29], to soft hydraulic continuum-style designs, such as the AMADEUS dexterous hand [30], an octopus inspired tentacle [31], and a soft robotic gripper for handling deep reefs [32]. Recently, a tendon-driven compliant hand was tested in the Mediterranean [28].

[3]Other technologies that use fluid flow for grasping include the Bernoulli gripper, commonly used to transport flat sheets; however, this technology expels, rather than aspirates, fluid. This technology was initially developed to astrictively grip and transport silicon wafers without contact [18].

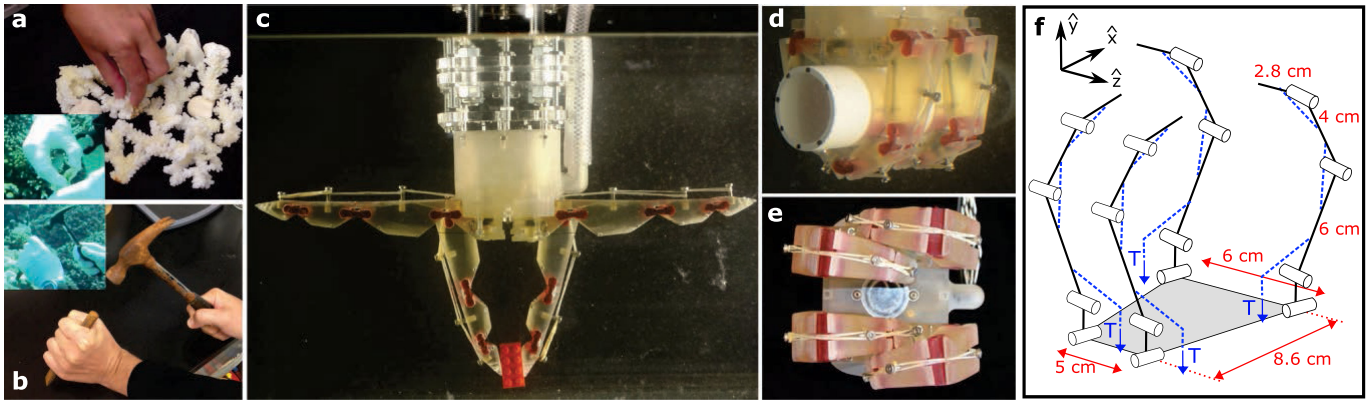


Fig. 2. RSRX hand utilizes underactuated tendon-driven fingers to perform both pinching and wrap grasping. These functions are important for sampling small objects—coral samples (a)—as well as larger objects and tools—chisel and hammer (b); these images are provided by the KAUST Reef Genomics Lab (C. R. Voolstra). This is replicated in the laboratory with a Lego block (c) and PVC tube (d). The finger flexure joints can twist and bend out of the plane of actuated finger motion. The offset finger placement on the palm (f) encourages the fingers to deflect laterally and slip past each other at large gripping forces, transitioning the hand from a pinch to an interlace wrap grasp (e).

As described by Kragten and Herder [20], the role of compliant hands is typically to grasp and hold objects, while the arms perform global manipulation tasks. Contact conditions influence how compliant hands settle around objects. The control of contact location, force, and friction using suction, therefore, provides a unique opportunity to improve the flexibility and robustness of underwater manipulation for this class of hand.

### A. *Pinching and Grasping*

Marine biologists at KAUST identified common tasks that divers perform in the field, such as using tools like a chisel and hammer to break coral samples free then delicately picking them up, as in Fig. 2(a) and (b). Accordingly, the compliant hand has the capability to both pinch with straight fingers and curl into a power grasp, demonstrated in Fig. 2(c) and (d). Each of the four fingers is driven by its own tendon and actuator (f). Two sets of fingers oppose each other, allowing for either two-finger or four-finger prismatic pinching. The actuators provide approximately 5.5-N maximum pinch force. Due to compliant flexure joints and staggered lateral spacing, the fixed-base fingers may twist past each other at lower pinch forces depending upon object shape and friction (e).

Joints with a nonlinear compliant behavior produce the desired finger curling behavior, from the base to the tip, as in Fig. 3(a). Elastic bands are stretched in order to create preload at each joint [see Fig. 3(a) and (c)], with the base joint having the smallest preload. As each joint curls, the effective moment arm of the extension spring diminishes, reducing overall stiffness. This arrangement ensures that the fingers are easy to close, reducing motor effort and improving grip strength. For more information about this mechanism and relevant stiffness modeling and characterization procedures, see [10] and [28].

In the current configuration, suction tubes protrude from the backs of the fingertips; the tubes are loosely coiled to reduce reaction forces as the fingers close, but they inhibit the ability of the hand to reach into tight spaces. Suction can alternatively be routed along the backs of the fingers with rubber tubing that doubles as springs to define finger curling mechanics [see Fig. 3(b)]. Coil springs inside the tubes keep them from collapsing so that flow is unaffected by finger posture. This approach to tube routing reduces the chance of snagging on the environment.

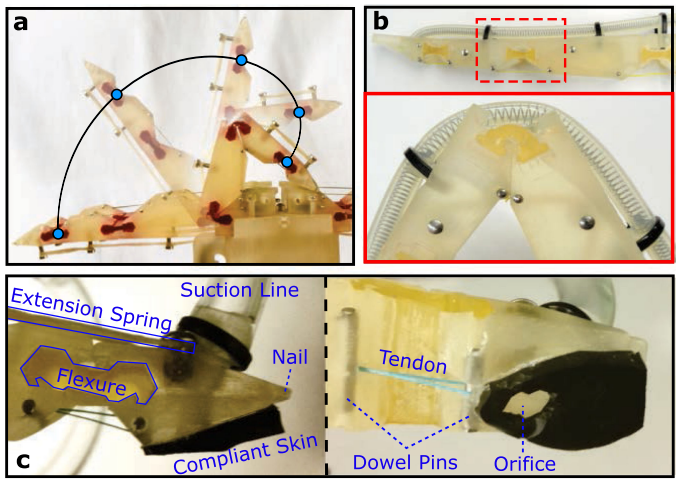


Fig. 3. Preloaded springs and flexures produce sequential curling without excessive stiffness [(a)–(c)]. A compliant suction line (b) becomes part of the spring mechanism, keeping the design compact. The suction orifice is located near the proximal end of the last phalanx and surrounded by a soft rubber skin (c). Fingernails can help underactuated hands picking up especially small objects [33]. Dowel pins reduce tendon friction.

### B. *Suction Implementation*

Suction is applied to through-holes from the back side of the finger, with tubing running up the hand to an external pump. The flow rate is kept relatively low to prevent disturbing the local environment, like stirring up sediment, or acquiring undesired objects in the vicinity. In comparison to suckers (e.g., [34]), this suction flow does not rely on forming a seal.

Pump selection, tube routing, and orifice design all influence the effectiveness of suction. For mobile applications, it is desirable to reduce the total robot mass and volume; therefore, suction pumps should be compact and, if possible, located at the robot body rather than in the hands. Positive displacement pumps can

produce a large suction pressure when the flow is restricted, but centrifugal pumps tend to be more compact for the same flow rate under most of the operating conditions. Given these considerations, the RSRX hand uses small centrifugal pumps (BLDC #DC40-2470) connected by flexible tubes to 21-mm$^2$ orifices at the fingertips. The system pulls 2.6 L/min of suction flow when the orifice is open and applies 1.2 N of force when clogged. Suction forces diminish if multiple tubes branch from a single inlet; therefore, each pump is connected to a single line (an alternative design could use valves to close lines not in use for a given task).

Previous work found that small changes in orifice location can have a disproportionate impact on suction effectiveness [10]. The orifice is located at the proximal end of the distal phalanx, as shown in Fig. 3(c). If the orifice is nearer to the tip, it may become easier to eject objects from a pinch, depending on fingertip and object geometry. This phalanx contact location also makes it easier to curl the distal phalanx in order to trigger pinch-to-wrap grasping transitions. A compliant skin around the orifice helps the edge of the orifice to comply with various surfaces and provides some damping, which reduces bouncing. With sufficient pressure, a very soft skin could allow the orifice to approximate a suction cup under blocked-flow conditions.

Debris or dirt can clog the suction orifice. In field deployment, a mesh shield should be placed over the orifice to prevent debris from jamming tubes or the pump. Monitoring suction flow strength can help detect when the lines must be purged, a strategy employed in some vacuum cleaners [35]. While suction lines are common for clearing silt, disturbing it can profoundly disrupt visibility. Therefore, it may be advised to turn OFF the pumps during particularly dirty digging tasks. Future versions of this hand should incorporate a way to clean the mesh (e.g., by reversing the flow to clear a clog) and explore the use of a venturi eductor[4] to protect the pump from fouling and damage.

## III. Modeling Hydrodynamic Forces

Hydrodynamic forces, including object drag and attractive suction flow, influence grasping. To simplify the analysis, we assume that suction forces and drag forces act independently on the object, and that flow disturbances arising from the slender fingers are negligible. These assumptions may break down for very small and light objects, respectively.

### A. Fluid Drag

A common model for object drag relates force magnitude $F_d$ to the square of flow velocity $v$, the projected area of the object in the flow plane $A$, fluid density $\rho$, and drag coefficient $C_d$ as follows:

$$F_d = \frac{1}{2}\rho v^2 C_d A. \tag{1}$$

When a cylinder moves with a moderate speed, such that Reynolds number (Re) ranges from $10^4$ to $10^6$, $C_d$ can be estimated as a constant value of 1.17 [38]. In the application of robotic grasping, where the fingertips move at a maximum speed of approximately 0.4 m/s relative to the palm and object sizes are usually at the 1–20-cm scale, Reynolds numbers will typically fall within or below this moderate range. At lower Reynolds numbers, $C_d$ scales linearly with object velocity such that $C_d \propto 1/\mathrm{Re}$ [39]. For humanoid robotic grasping, drag forces at these low velocities are small compared with inertial, contact, and suction forces. Therefore, a constant value for $C_d$ is assumed knowing that drag will be underestimated at low velocities.

[4]A device similar to a venturi ejector [36], a common tool used by marine archaeologists for dredging (removing sediment) and revealing artifacts [37].

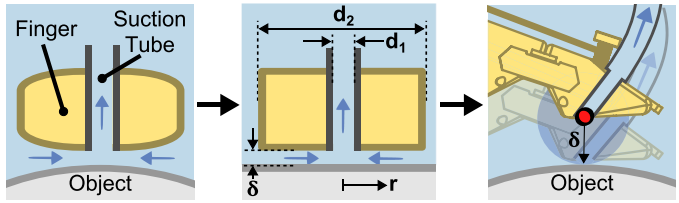


Fig. 4. For distances of a few millimeters, local geometry is assumed to approximate two flat plates. The fingertip with a width of $d_2$ includes a suction orifice with diameter $d_1$. Suction force is a function of the distance between the fingertip and object $\delta$. It is estimated by assuming inviscid antisymmetric flow about the orifice and integrating pressure over the surface of the fingertip as a function of radius $r$.

### B. Suction Flow

Suction flow will attract nearby objects, as a function of flow rate and distance from the orifice. When the object is far from the fingertip, flow generated in the vicinity of the hand will create an attractive drag force on the object; at the gentle flow scales implemented in this work, the force will be small compared to flow generated by other local water currents. At intermediate distances, on the order of centimeters and millimeters, pressure drop due to motion of fluid moving between the surface of the object and finger will dominate. At very small distances, hundreds of micrometers, viscous effects will start to contribute significantly to suction force, and the pump will become increasingly restricted. When the orifice is completely closed, the pump will apply a static pressure which we assume is the maximum possible suction force.

A flat-plate model with a single inlet pipe is used to approximate the intermediate distance range, as shown in Fig. 4; it is assumed that the gap between the object and the fingertip $\delta$ is small compared to local radii of curvature. Assuming inviscid flow and ignoring gravitational effects, Bernoulli's equation can be applied in order to calculate line pressure at a given radial distance from the center of the orifice $r$, where $Q$ is the volumetric flow rate and $\rho$ is the mass density of water. Integrating pressure over the plate's surface, from the inner orifice, $d_1/2$, to the edge of the fingertip, $d_2/2$, allows us to estimate the suction force

$$F_{s,1}(Q,\delta) = \frac{Q^2\rho}{4\pi\delta^2}\left(\ln\frac{d_2}{d_1}\right). \tag{2}$$

Equation (2) approaches zero as the distance decreases, and the flow is restricted. Another suction force must be considered that comes from the pressure applied by the pump $P$ over the area

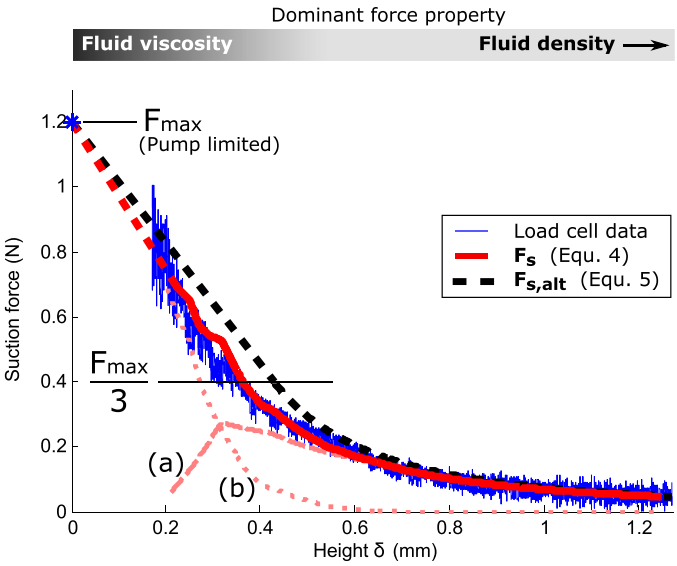


Fig. 5. Suction force is measured experimentally and compared with the estimates. (a) Force model due to Bernoulli flow $F_{s,1}$ given measured values of flow rate. (b) Force component $F_{s,2}$ due to measured orifice pressure. For small gaps, fluid viscosity dominates; further away, fluid density and inertia dominate. The red line, $F_s$, is the addition of (a) and (b). A single $F_{\max}$ point is experimentally measured with a hand-held force scale (blue star), and a red dashed line predicts an approximate suction force for distances less than 200 $\mu$m. $F_s$ is similar to the load cell suction force measurement (blue line). A simplified model, $F_{s,\text{alt}}$ (black dashes), requires just two input parameters: maximum pump flow rate and maximum suction pulloff force – 2.6 L/min and 1.2 N, respectively.

of the orifice as

$$F_{s,2}(P) = \frac{\pi}{4} d_1^2 P. \tag{3}$$

For a simplified model, we can superimpose these effects to estimate the overall suction force for the rates and dimensions in humanoid robotic grasping as

$$F_s = F_{s,1} + F_{s,2}. \tag{4}$$

Fig. 5 compares the model estimate with measurements for a range of distances. As the distance between the fingertip and a flat plate decreases, the flow rate drops and orifice pressure rises. These variables are measured then used to calculate $F_s$ with (4) (solid red line); the result matches load cell readings (blue line). Experimental data are excluded for distances less than 200 $\mu$m, at which point small amounts of flexibility and vibration in the experimental setup make it increasingly difficult to obtain accurate results. Viscous effects become important in this range but are not included here. Instead, we observe that a straight line (red dashes) extending to the point of blocked-flow fits the empirical data relatively well. This single maximum suction pressure point is measured independently when the fingertip is in full contact.

The method proposed thus far requires knowledge of the pump flow–pressure characteristics, which will change with pump parameters and tubing/orifice implementation. For a simpler model that requires less measurement, we can assume constant flow at large and intermediate distances, until the Bernoulli suction estimate becomes tangent with a line extending from the maximum suction force corresponding to blocked flow. This

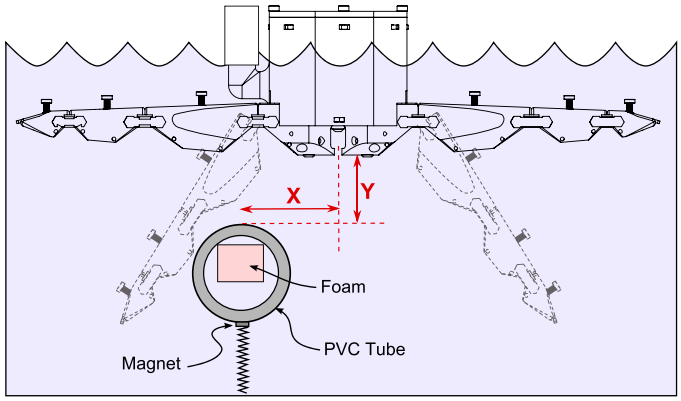


Fig. 6. Experimental grasp region is determined for a PVC tube. Foam inside the tube makes it approximately neutrally buoyant. Very light magnets and springs locate the tube inside a water tank. $X$ and $Y$ coordinates are defined from the center of the hand, when the object is in contact with the palm. The hand is closed in 1 s, and the grasp is recorded as a success or failure.

model, $F_{s,\text{alt}}$, is shown with a black dashed line and also matches the data, while requiring only two measurements, i.e., blocked suction pressure and free flow rate:

$$F_{s,\text{alt}} = \begin{cases} F_{s,1}(Q = Q_{\max}), & \delta \geq \delta_t \\ F_{\max}\left(1 - \dfrac{2\delta}{3\delta_t}\right), & \delta = (0, \delta_t) \\ F_{\max}, & \delta \leq 0 \end{cases}. \tag{5}$$

The transition distance $\delta_t$, when the suction force is $F_{\max}/3$, is

$$\delta_t = \sqrt{\frac{3\rho Q_{\max}^2}{4\pi F_{\max}} \ln\left(\frac{d_2}{d_1}\right)}. \tag{6}$$

Dynamic simulations utilize this model to estimate the contributions of the maximum pump pressure and the maximum flow rate on multifinger grasping with suction under water.

## IV. Object Acquisition

In subsea environments, station keeping can be difficult for floating-base robots, and buoyant objects can move in water currents. Teleoperators may want to grasp quickly, when the hand is in position and before items float away. These concerns motivate the consideration of inertial forces and hydrodynamic drag during rapid grasping.

### A. Dynamic Grasp Model Validation

The grasp region was tested in a still water tank, as shown in Fig. 6. The hand was located relative to a neutrally buoyant 48-mm 110-g PVC tube with 5-mm minimum spatial resolution. Each location was tested for three independent trials, with successful grasping averages represented by dot size in Fig. 7. Without suction (white), there is a large region around the center of the palm that always results in a successful grasp. Near the edges, success becomes irregular, likely because the springs that hold the tube in place are very soft and flexible, so there is some variability in initial tube position and orientation.

Due to sensitivity to minor differences in initial position and orientation, mapping the entire grasp region is slow. Therefore,

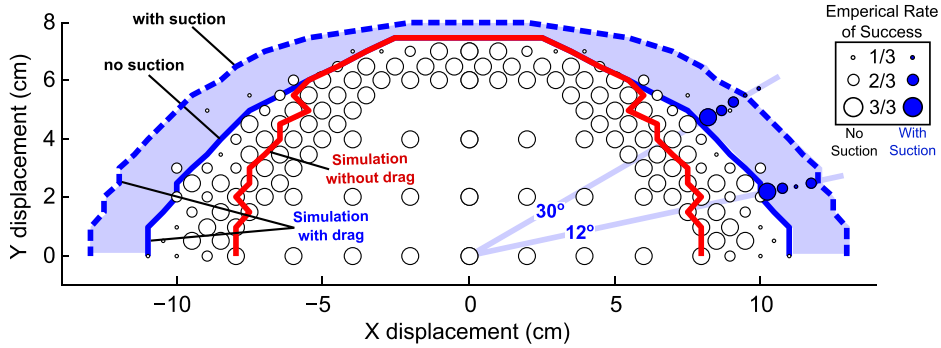


Fig. 7. Experimental (dots) and simulated (outlines) grasp trials collected at 5-mm resolution help to validate SimGrasp representation of dynamic grasping under water. Each location in half of the grasp region is tested three times; results are mirrored for clarity. Dot size indicates the percentage of success. The simulation with water drag included (blue) matches expected experimental trends.

two vectors, corresponding to 12° and 30° measured anticlockwise from the palm as shown in Fig. 7, were chosen for more detailed investigation of the effects of suction flow. Each blue circle corresponds to three trials with approximately the same starting location. In collecting results at these peripheral locations, we observed that grasping with suction is sensitive to initial orientation of the object out of the plane of finger motion. At times, suction on only one finger engaged with the object, pulling it into the hand but not into a power grasp. In some situations, this atypical grasp may be acceptable for acquiring an object, but it will not afford as much strength.

Dynamic numerical simulations were conducted and compared with experimental results. The RSRX hand was modeled in SimGrasp [22] as shown in the kinematic diagram of Fig. 2(f) including the phalanx geometry and estimated nonlinear joint stiffnesses. Suction flow was added between the finger and the object using (5), applied from the center of the finger-pad orifice to the closest point on the object's surface, as in Fig. 4. Drag was also implemented on the object using (1). In simulation, the finger tendons were given a controlled speed to close the fingers completely in $\approx 1$ s.

Three different cases were simulated: without any hydrodynamic forces (red), with only fluid drag (blue, solid), and with both suction and fluid drag (blue, dashed). Fluid drag on the object is necessary to match the grasp regions found experimentally and increases the grasp region.[5] Suction increases the grasp region area by 34%.

### B. Object Inertia

Intuitively, the effect of suction flow diminishes as object mass increases—as the magnitudes of flow forces are dwarfed by inertial and contact forces. The question remains: At what object mass is it no longer useful to employ gentle suction? The grasp region of the hand was explored using SimGrasp, with a spatial resolution of 1 cm for different object masses: 100 g, 1 kg, and 10 kg. Results are shown in Fig. 8. The lightest object (blue) produces the largest overall grasp region, both with and without suction. The 10-kg object (black) sees no change in the grasp region with the addition of suction. The intermediate mass

[5]In this regard, grasping a buoyant object under water may be easier than grasping objects floating in space.

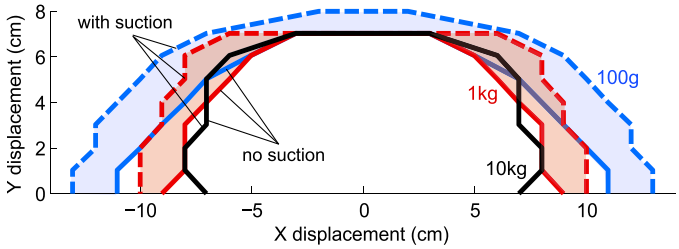


Fig. 8. Grasp regions computed with 1-cm resolution for 100-g (blue), 1-kg (red), and 10-kg (black) cylinder with a diameter of 6 cm. Solid lines indicate grasp regions without suction flow; dashed lines are with fingertip suction. Shaded regions highlight improvement due to suction.

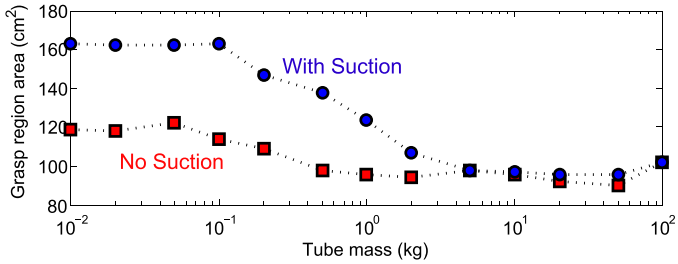


Fig. 9. As a cylindrical object increases in mass, but remains the same size, the influence of suction on grasp region diminishes. For this implementation, suction has no notable effect over 2 kg.

(red) sees a substantial increase in the grasp region with suction. Note also that the region for this mass is less regular than for the 100-g object, as the results are sensitive to details of the contact conditions and underactuated hand closing behaviors.

Fig. 9 plots the overall area of the grasp region, with and without suction, as a function of increasing object mass. The effect of suction is substantial when the object mass is below 2 kg, a range that captures many relevant objects for humanoid grasping. The robot Ocean One is approximately 200 kg, meaning that suction would play a negligible role when the platform tries to ground itself by grasping stationary structures. The overall grasp region of the hand, and attractive effect due to suction, plateaus for objects less than 100 g; at this mass, maximum drag becomes an order of magnitude greater than object inertia. Note that this model does not account for complex flows induced by finger motion, which could especially influence light objects.

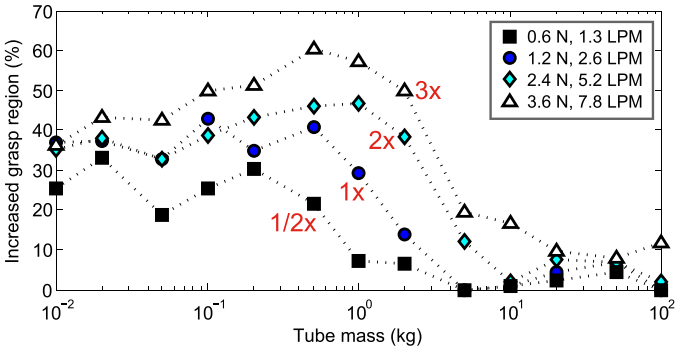


Fig. 10. Percentage increase in the grasp region with changes in the maximum static pump pressure and flow rate. For reference, the pump on the RSRX hand is designated as "1x." Increasing maximum suction force and flow rate has a nonlinear influence, most greatly affecting objects between 500 g and 2 kg. Gentle suction forces can provide a significant benefit for light objects.

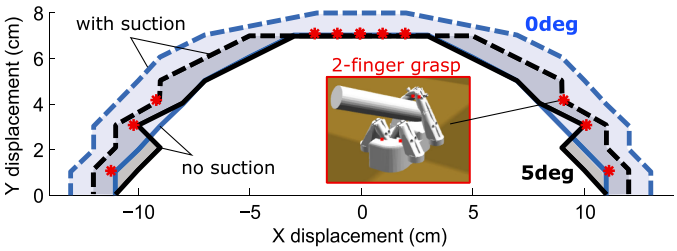


Fig. 11. Grasp regions computed with 1-cm resolution for a 100-g cylinder with a diameter of 6 cm. The blue lines represent simulations where the object is initially oriented to approximate planar grasping; the axis of the cylinder is orthogonal to the plane of finger motion. The black lines represent regions of trials, where the object's initial orientation includes 5° of rotation about the $+\hat{x}$-direction. Solid lines bound initial object locations from which the object settles into a grasp without suction and dashed lines bound regions with fingertip suction flow. The red asterisks are locations where the tube settles in a two-finger grasp.

### C. Suction Intensity

Fig. 10 describes the improvement of grasp region with varying suction flow conditions. The line designated as "1x" represents the data from Fig. 9 and pump parameters for the RSRX hand. As expected, increasing the pump flow rate and maximum pressure improves the influence of suction. However, this change is not linear with object mass. Cylinders with intermediate masses (500 g–2 kg) are most sensitive to changing suction parameters. Intuitively, aggressive suction will be needed to extend the grasp region of the most massive objects. However, light or moderate suction is effective for object masses commonly encountered.

### D. Object Motion Out of the Grasping Plane

The model developed in SimGrasp captures three-dimensional dynamics. Thus far, planar grasping is approximated by performing symmetric finger motions and initiating each trial with the tube's long axis orthogonal to the grasping plane. This idealized case, shown in blue in Fig. 11, does not capture uncertainty in the object's orientation.

In order investigate sensitivity to imperfect alignment between the hand and object, simulations are initiated with the cylinder's long axis tilted 5° about the $+\hat{x}$-direction, defined in Fig. 2(f). For each possible starting location, the simulation determines whether the cylinder will be pulled into the palm. The boundary of the acquisition region is evidently larger with suction flow, both for the aligned and slightly misaligned initial conditions. The shape of the region without suction and with misalignment reflects the statistical trends observed in experimental trials, as shown in Fig. 7. The effect of suction flow on the grasp region reduces with rotational misalignment. Interestingly, for the perturbed initial conditions, the grasp can evolve to a stable asymmetric two-fingered grasp, highlighted with red asterisks and visualized in the inset in Fig. 7. These cases tend to occur near the edges of the acquisition region. As noted in Section IV-A, this behavior was observed during experimental trials.

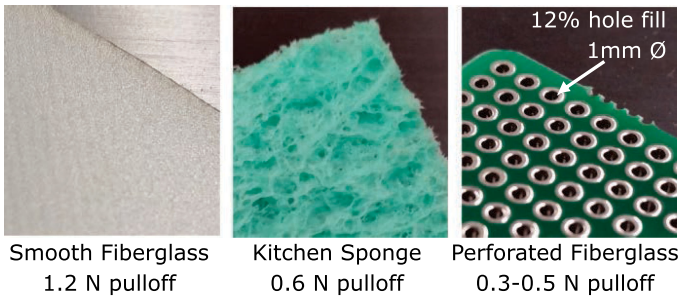


Fig. 12. Normal force applied by suction to a flat surface is sensitive to porosity and rugosity. The pull-off force is highest for smooth, flat surfaces and lower for highly porous and perforated surfaces.

## V. Grasp Security

The objects that one might want to grasp range from small pieces of coral to large pieces of equipment. They have a wide range of surface profiles, from smooth to rough, and they may be porous, or coated with biofilm or mud. In this section, we explore the ability of gentle suction flow to improve grasp security when object surface properties are unpredictable. We focus on fingertip pinch grasps [e.g., Fig. 2(c)], which are particularly dependent on friction conditions at the contacts. *Security* is defined here in terms of the maximum sustainable external force pulling away from the palm.

### A. Material and Surface Properties

For smooth objects, the orifice can be entirely blocked. For the RSRX system, this results in a 1.2-N normal pull-off force, tested by allowing suction to fully engage with a neutrally buoyant piece of the material and then pulling it off with a force scale normal to the fingertip's surface. For porous and rough objects, the pull-off force decreases, but it remains noticeable even for materials like sponge and a perforated panel with 1-mm-diameter holes filling 12% of the area (see Fig. 12). While the pull-off force is consistent for the smooth fiberglass and kitchen sponge, it varies between tests on the perforated fiberglass likely due to variation in alignment between the hole pattern and the 5-mm-diameter fingertip orifice. Although these materials do not encapsulate the full variety of objects found in

TABLE I
FRICTION COEFFICIENTS BETWEEN A BARE FINGERTIP AND ACRYLIC OR SANDPAPER IN AIR, IN WATER, AND IN WATER WITH SUCTION (± STANDARD DEVIATION REPRESENTED AS A PERCENTAGE OF THE AVERAGE)

| | Acrylic | | Sandpaper | |
|---|---|---|---|---|
| | Static | Dynamic | Static | Dynamic |
| Air | 0.51 ±3.9% | 0.21 ±4.7% | 0.85 ±6.0% | 0.56 ±6.0% |
| Water | 0.34 ±5.8% | 0.20 ±5.9% | 0.76 ±4.3% | 0.58 ±1.5% |
| Suction | 0.40 ±8.1% | 0.23 ±4.2% | 1.16 ±14.9% | 0.93 ±19.9% |

marine environments, they do allow us to start understanding how suction flow affects disparate surfaces.

Improving friction can make pinching significantly more reliable. In fact, humans continuously monitor fingertip friction in pinching tasks [40]. Suction can affect the maximum shear stress at a contact. Experiments capture the effect of water lubrication and improved traction. Static and dynamic coefficients of friction were measured for a Visijet Crystal 3D printed fingertip on two materials, acrylic and 1500 grit sandpaper, chosen to represent slippery and high-friction flat surfaces, respectively. The fingertip was aligned with the surface, producing mostly blocked flow, but without a soft skin sealing was imperfect. Averages from five trials in air, water, and water with suction flow are reported in Table I.

In general, water decreases the static coefficient of friction slightly, while the dynamic coefficient remains nearly unchanged. In both material cases, suction improves the coefficient of friction under water. This increase is most pronounced with the fine sandpaper, at 53% static and 60% dynamic, respectively. Acrylic friction increases by 17% and 15% for static and dynamic cases, respectively. In interpreting these results, it should be acknowledged that tribology in saltwater, with or without contact motion and suction flow, is a complex phenomenon, and some variability in the measured ratio of tangential to normal force (used to obtain the coefficient of friction) is expected. Variability is most noticeable for sandpaper with suction, where details of sealing around the orifice appear to produce substantial effects. A more detailed study of undersea contact tribology is a topic for future investigation, especially during rapid contact. The results in Table I are relevant to investigate how changes in contact friction under water affect the security of a pinch grasp after acquisition. Note that simulations in Section IV exclude the apparent change in the coefficient of friction due to suction.

### B. Application to Pinching: Object Size

Straight-finger pinching is an important function of the RSRX hand, when the fingers cannot wrap around very small or large objects. The primary point of contact with the object will be at the fingertips; therefore, suction plays an important role in force closure or the ability to constrain object motion with frictional contact forces even when form closure is not achieved [41]. In the presence of an external pullout force $\overrightarrow{F_e}$, pinch security will be influenced by friction $\overrightarrow{F_f}$, normal contact force $\overrightarrow{N}$, and suction force applied to the object $\overrightarrow{F_s}$, as modeled in Fig. 13(a). Changing the vertex angle $\alpha$ affects both the object size and finger orientations, assuming flat fingertip contact.

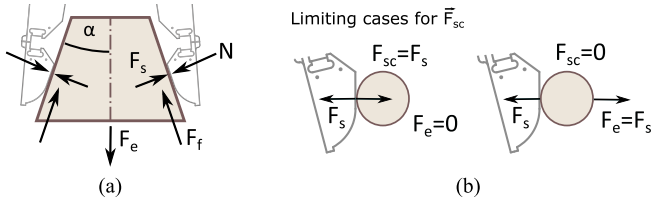


Fig. 13. (a) Pinch model includes object size $\alpha$, normal force $N$, suction force $F_s$, friction $F_f$, and external pullout force $F_e$. (b) Contribution of contact force due to suction $F_{sc}$ changes with external load, illustrated in this one-dimensional case where $F_a = 0$.

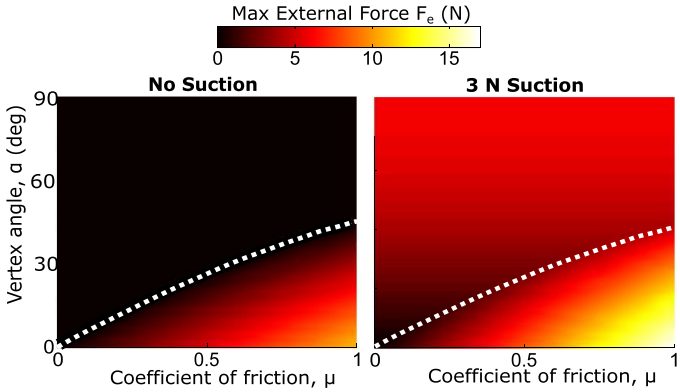


Fig. 14. Maximum external force magnitude $F_e$ (color bar) is influenced by object properties like coefficient of friction and object vertex angle $\alpha$. Suction flow makes a large difference unless both friction and object angle are low. White dotted lines separate cases when the maximum external force occurs at maximum squeeze force from cases when it occurs with zero squeeze force.

With a friction coefficient such that $F_f = \mu N$, the force balance for the triangular object in the vertical direction is

$$F_e = 2\,[F_s\,\sin\alpha + N(\mu\,\cos\alpha - \sin\alpha)]. \tag{7}$$

Normal force is a function of hand actuation $\overrightarrow{F_a}$ and contact force due to suction $\overrightarrow{F}_{\rm sc}$, which is bounded by maximum pump pressure

$$\overrightarrow{N} = \overrightarrow{F_a} + \overrightarrow{F}_{\rm sc}, \quad F_{\rm sc} = [0, F_s]. \tag{8}$$

As demonstrated in Fig. 13(b) for a one-dimensional case when $\overrightarrow{F_a} = 0$, suction force applied to the object $\overrightarrow{F}_s$ remains constant during contact, but normal force changes with external load. We assume that suction flow does not apply an adhesive contact force and that fingers align flush with the surface to provide maximum suction when the orifice is sealed.

The influence of suction over multiple friction coefficients and object sizes is demonstrated in Fig. 14. When attempting to maximize external force resistance, there will be a critical angle $\alpha_c = \tan^{-1}(\mu)$ below which squeeze force and friction should be maximized, but above which squeeze force should be minimized and failure will occur after $F_{\rm sc}$ reaches 0 N. Without suction, no object can be grasped above the critical angle (white dashed line). With suction, any object can be acquired except for very slippery objects with small vertex angles. In the region with large object sizes, the force resisted by the hand is independent of the friction coefficient.

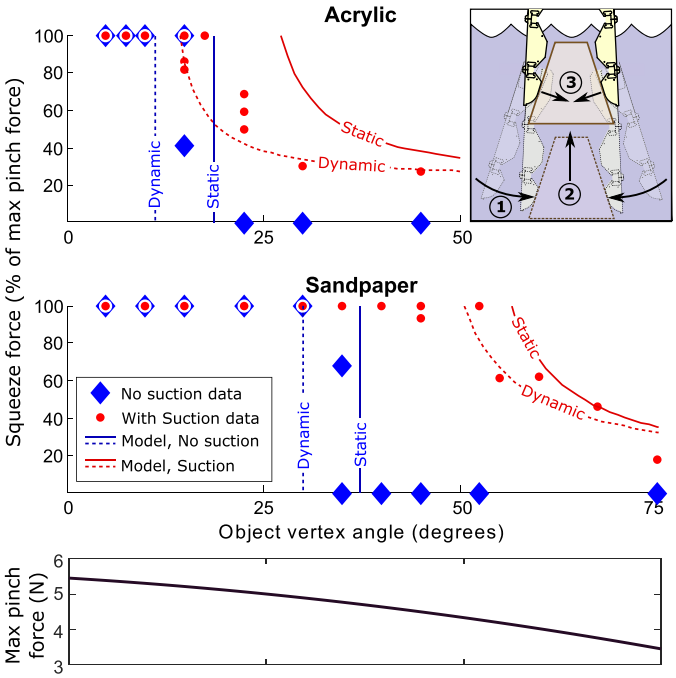


Fig. 15. Security of a pinch changes with object vertex angle, grasp force, and material properties. Predicted pinch forces, defined as a percentage of maximum available for a given actuator, are plotted for static and dynamic friction using (7). Vertical blue lines indicate maximum object vertex angles for static and dynamic friction, without suction. Red curves indicate the limiting cases with suction. Blue diamonds and red dots show empirical limits without and with suction. There were roughly 60 grasp trials in total. Predictions using the dynamic coefficient of friction give a better, mostly conservative fit. Inset shows grasping sequence: (1) fingers close on object; (2) they apply a gentle ≈1 N pinch and attempt to lift the object; and (3) if lifting succeeds, the grasp force increases incrementally until failure. Due to nonlinear joint actuation, maximum pinch force changes with object size.

This simple model can also determine when a grasp will fail due solely to excessive pinch force and is confirmed with experiments. This is a concern with suction on objects larger than the critical angle $\alpha_c$. In a tank of water, neutrally buoyant triangles of various sizes are picked up by the hand using a minimal grasp force or suction, as shown in the inset in Fig. 15. The grasp force is incrementally increased until either maximum actuator torque is reached or the grasp fails. The tendon force on the finger, used to compute the pinch force, is measured using a cantilevered magnet mechanism that deflects under tension and a Hall-effect sensor built into the finger. Sensor details can be found in [11]; estimated accuracy in the pinch force is approximately $\pm 0.3$ N. The results, shown in Fig. 15, are compared with the model predictions using the friction coefficient mean values in Table I. Maximum grasp force changes with finger pose, as tendon and spring moment arms at the proximal joint change during finger motion; maximum pinch force is normalized for each finger pose (corresponding to the object apex angle).

As seen in Fig. 15, there is relatively good agreement between the simple model and empirical observations. Without suction, the transition from maximum successful grasp force to failure is sudden and occurs between the corresponding estimated critical angles $\alpha_c$ for the dynamic and static coefficients of friction. As the grasping force increases, there are inevitably some disturbances at the contacts due to the compliant nature of the hand. Consequently, the dynamic coefficient of friction is usually in effect. With suction, the data again fall closer to the predictions using the dynamic coefficient of friction. As predicted, the limiting object vertex angle is much higher. It should be noted that although suction helps to pull the fingers into alignment with the object surface, some trials may have slight misalignments that make suction less effective. This model can help robot teleoperators to limit grasping forces of large smooth objects, based on hand pose and estimated suction engagement.

## VI. Discussion

Suction flow at the fingertips is effective for improving object acquisition and pinch security when grasping under water. In particular, it expands the outer edges of the hand's grasp region for light to moderately massive buoyant objects (less than ≈2 kg). This means that it can be helpful for tasks including the manipulation of, for example, tools. Suction also increases grip security on objects of almost all shapes and sizes, as long as suction is engaged at the contact. A few other advantages of grasping with gentle suction flow are apparent.[6]

1) *Gentle handling of slippery objects:* Fig. 1 shows the RSRX hand pinching a bar of soap, a case that might be analogous to an object covered in slimy biofilm. Without suction, the pinch invariably failed in one of two ways: 1) the bar slipped and ejected out of the hand; or 2) the fingernails engaged the surface but the grasp was imprecise and unstable. Suction is a solution for pinching gently without fingernails or spikes that could damage the surface of the soap bar.
2) *Capture of erratic small targets:* Orifice location helps determine where on the hand objects are likely to settle; suction creates a low-energy target. This is especially meaningful for small objects that are difficult to capture because they require more accurate hand positioning and are sensitive to even light currents. In order to demonstrate this concept, a 2-g standard Lego piece, that is weighted to be approximately neutrally buoyant, is pulled into the fingertip by suction flow, as shown in Fig. 16. The location of the orifice is such that the object is in a convenient place for pinching. Without suction, it would be difficult to accurately track this floating item. This technique could be useful for the capture of small swimming sea creatures as well. The shape of a free-floating object will influence how it settles on a suction fingertip. For example, we observe instability during edge contact with a neutrally buoyant block, as in Fig. 17(a); the block will reorient such that a flat face is flush with the fingertip within a couple seconds from initial contact. The time scale and direction of reorientation depend on local flow disturbance on the object as well as suction engagement. Alternatively, vertex contact is stable, as in Fig. 17(b), though the object can reorient when a second finger applies internal pinch

[6]A video submission accompanies this work, demonstrating dynamic grasping of a PVC tube, as well as the additional cases described in this section.

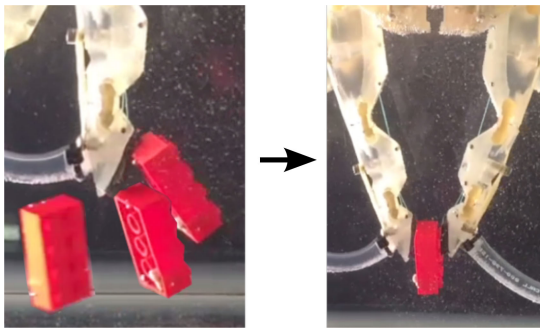

Fig. 16. Especially for very small objects, suction can significantly change the strategy when attempting a pinch. There may be a fish-and-wait phase before performing a pinch, shown here with a neutrally buoyant Lego block.

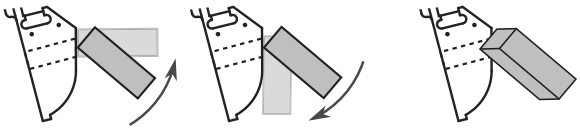


Fig. 17. Edge contact between a suction fingertip and a block is not a stable pose. Over time, on the order of a couple seconds or less, a small block will reorient such that a flat side is flush with the fingertip's surface (a). However, the contact can be stable if a convex feature, such as the vertex of a block, enters the orifice (b).

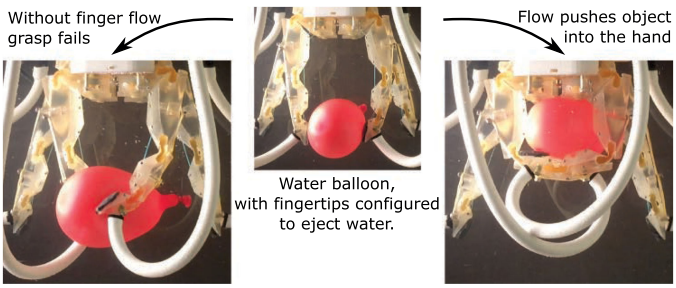


Fig. 18. Reverse flow, configured to push objects away from the fingertips, can enable new behaviors. In this case, a water balloon is pinched gently. If the hand attempts to pull the balloon into the hand, the grasp fails due to pinch instability. Instead, reverse flow can briefly reduce the finger/object friction, allowing the object to slide into the palm without opening the hand or relaxing the grasp.

forces, as observed in Fig. 16. Future work could characterize how suction flow, manipulator behavior, and fingertip geometry encourage contact orientations of various floating object shapes.

3) *In-hand manipulation with reverse flow:* Reversing flow can push the fingertips and object away from each other, temporarily decreasing friction. This is particularly interesting in the case of triggering in-hand manipulation events, for example, transitioning from a pinch to a wrap grasp. It is an alternative to squeezing while dithering the grasp force or pushing the object against the environment while briefly loosening the grasp [42]. Soft sea creatures, approximated in Fig. 18 by a water balloon, pose a special challenge: squeezing harder causes pinch failure, and releasing the grip risks losing the object. A brief reverse flow pushes the balloon in a somewhat predictable way into the hand. Other possible uses for reverse flow include evacuating clogged suction lines or gently clearing an area of silt or sand to increase visibility.

## VII. Conclusion

Grasping is strongly dependent on finger–object contact conditions. This is particularly true for compliant underactuated hands, where friction determines how fingers will settle on the object. Gentle suction flow provides a way to modify the contact conditions directly. For light objects, suction adds an attractive force that aids in acquisition and grasp security. For medium and heavy objects, the direct force is negligible, but suction increases the coefficient of friction, which, in turn, increases the security of pinching. Unlike suction cups, suction flow works on rough and porous objects, as well as smooth ones. Because the suction flow in this work is gentle, the effect on dynamic grasping and static holding is sensitive to small changes in object–hand and surface–orifice misalignments respectively.

The effects of gentle suction flow are often nonlinear and, except for special cases, difficult to predict with simple models as they depend on interactions among the contacts, water currents, and hand compliance and kinematics. Therefore, a dynamic simulation such as SimGrasp [22] that can incorporate the effects of suction flow is useful for exploring various grasping scenarios and design parameters, such as flow rate and static pump pressure. Despite these complexities, suction flow is generally beneficial both for acquiring and retaining objects ranging from delicate sea creatures to rocks and tools.

### A. Future Work

Suction could turn ON and OFF during complex manipulation tasks; future work should address interfacing suction control with the operator. Taking inspiration from fish and other animals, short bursts of suction may be more intuitive than turning it ON continuously. The control of suction flow could be accompanied by flow and pressure sensing. Because these variables depend strongly on the degree of restriction at the orifice, they also provide a kind of tactile sensing [11].

Underwater manipulator designs can consider additional suction parameters. For example, although we focused on fingertip orifices, future work could apply suction at other locations, like the palm. Given many suction flow orifices, alternate pump and valving systems could control their behavior in a network. Finally, tribology with suction is a complex subject but will ultimately provide a more complete understanding of the effects of suction flow, with and without relative motion between contacting fingertips and objects.

## Acknowledgment

The support of the members of the Biomimetics and Dexterous Manipulation Lab and the Stanford AI Lab is gratefully acknowledged. Any opinions, findings or conclusions expressed in this material are those of the authors and do not necessarily reflect the views of the funding sources.

## REFERENCES


[1] O. Khatib *et al.*, "Ocean One: A robotic avatar for oceanic discovery," *IEEE Robot. Automat. Mag.*, vol. 23, no. 4, pp. 20–29, Dec. 2016.

[2] G. Antonelli, T. I. Fossen, and D. R. Yoerger, *Modeling and Control of Underwater Robots*. Cham, Switzerland: Springer, 2016, pp. 1285–1306.

[3] F. Zhang, G. Marani, R. N. Smith, and H. T. Choi, "Future trends in marine robotics [TC spotlight]," *IEEE Robot. Automat. Mag.*, vol. 22, no. 1, pp. 14–122, Mar. 2015.

[4] J. Evans, P. Redmond, C. Plakas, K. Hamilton, and D. Lane, "Autonomous docking for Intervention-AUVs using sonar and video-based real-time 3D pose estimation," in *Proc. IEEE Oceans: Celebrating the Past ... Teaming Toward the Future*, 2003, pp. 2201–2210.

[5] P. J. Sanz *et al.*, "TRIDENT An European project targeted to increase the autonomy levels for underwater intervention missions," in *Proc. IEEE Oceans: San Diego*, 2013, pp. 1–10.

[6] G. Marani, S. K. Choi, and J. Yuh, "Underwater autonomous manipulation for intervention missions AUVs," *Ocean Eng.*, vol. 36, pp. 15–23, 2009.

[7] T. E. Higham, S. W. Day, and P. C. Wainwright, "Multidimensional analysis of suction feeding performance in fishes: Fluid speed, acceleration, strike accuracy and the ingested volume of water," *J. Exp. Biol.*, vol. 209, no. 14, pp. 2713–2725, 2006.

[8] M. Muller, J. Osse, and J. Verhagen, "A quantitative hydrodynamical model of suction feeding in fish," *J. Theor. Biol.*, vol. 95, no. 1, pp. 49–79, 1982.

[9] M. C. de Jong, J. Sparenberg, and J. De Vries, "Some aspects of the hydrodynamics of suction feeding of fish," *Fluid Dyn. Res.*, vol. 2, no. 2, pp. 87–112, 1987.

[10] H. S. Stuart, S. Wang, B. Gardineer, D. L. Christensen, D. M. Aukes, and M. R. Cutkosky, "A compliant underactuated hand with suction flow for underwater mobile manipulation," in *Proc. IEEE Int. Conf. Robot. Automat.*, 2014, pp. 6691–6697.

[11] H. S. Stuart *et al.*, "Suction helps in a pinch: Improving underwater manipulation with gentle suction flow," in *Proc. IEEE/RSJ Int. Conf. Intell. Robots Syst.*, 2015, pp. 2279–2284.

[12] G. J. Monkman, "An analysis of astrictive prehension," *Int. J. Robot. Res.*, vol. 16, no. 1, pp. 1–10, 1997.

[13] N. Correll *et al.*, "Analysis and observations from the first amazon picking challenge," *IEEE Trans. Automat. Sci. Eng.*, vol. 15, no. 1, pp. 172–188, Jan. 2018.

[14] C. Hernandez *et al.*, "Team Delft's robot winner of the Amazon Picking Challenge 2016," in *Proc. Robot World Cup*, 2016, pp. 613–624.

[15] S. Hasegawa, K. Wada, Y. Niitani, K. Okada, and M. Inaba, "A three-fingered hand with a suction gripping system for picking various objects in cluttered narrow space," in *Proc. IEEE/RSJ Int. Conf. Intell. Robots Syst.*, 2017, pp. 1164–1171.

[16] K. Yamaguchi, Y. Hirata, and K. Kosuge, "Development of robot hand with suction mechanism for robust and dexterous grasping," in *Proc. IEEE/RSJ Int. Conf. Intell. Robots Syst.*, 2013, pp. 5500–5505.

[17] N. C. Dobson, "Developmental deep-water archaeology: A preliminary report on the investigation and excavation of the 19th-century side-wheel steamer SS Republic, lost in a storm off Savannah in 1865," in *Proc. IEEE Oceans*, 2005, pp. 1761–1769.

[18] J. Paivanas and J. Hassan, "Air film system for handling semiconductor wafers," *IEEE IBM J. Res.* , vol. 23, no. 4, pp. 361–375, 1979.

[19] A. M. Dollar and R. D. Howe, "Towards grasping in unstructured environments: Grasper compliance and configuration optimization," *Adv. Robot.*, vol. 19, no. 5, pp. 523–543, 2005.

[20] G. A. Kragten and J. L. Herder, "The ability of underactuated hands to grasp and hold objects," *Mech. Mach. Theory*, vol. 45, no. 3, pp. 408–425, 2010.

[21] D. M. Aukes, "Design and analysis of selectively compliant underactuated robotic hands," Ph.D. dissertation, Dept. Mech. Eng., Stanford Univ., Stanford, CA, 2013.

[22] S. Wang, "SimGrasp: Grasp Simulation Package," BitBucket, 2017. [Online]. Available: https://bitbucket.org/shiquan/sim-grasp

[23] K. Hauser, "Robust contact generation for robot simulation with unstructured meshes," in *Proc. Int. Symp. Robot. Res.*, 2016, pp. 357–373.

[24] L. Birglen, T. Laliberté, and C. Gosselin, *Underactuated Robotic Hands* (Springer Tracts in Advanced Robotics), vol. 40. New York, NY, USA: Springer, 2007.

[25] A. M. Dollar and R. D. Howe, "The highly adaptive SDM hand: Design and performance evaluation," *Int. J. Robot. Res.*, vol. 29, no. 5, pp. 585–597, 2010.

[26] C. Melchiorri, G. Palli, G. Berselli, and G. Vassura, "Development of the UB hand IV: Overview of design solutions and enabling technologies," *IEEE Robot. Automat. Mag.*, vol. 20, no. 3, pp. 72–81, Sep. 2013.

[27] M. G. Catalano, G. Grioli, E. Farnioli, A. Serio, C. Piazza, and A. Bicchi, "Adaptive synergies for the design and control of the pisa/iit softhand," *Int. J. Robot. Res.*, vol. 33, no. 5, pp. 768–782, 2014.

[28] H. Stuart, S. Wang, O. Khatib, and M. R. Cutkosky, "The ocean one hands: An adaptive design for robust marine manipulation," *Int. J. Robot. Res.*, vol. 36, no. 2, pp. 150–166, 2017.

[29] A. Aggarwal, P. Kampmann, J. Lemburg, and F. Kirchner, "Haptic object recognition in underwater and deep-sea environments," *J. Field Robot.*, vol. 32, no. 1, pp. 167–185, 2015.

[30] D. M. Lane *et al.*, "The AMADEUS dextrous subsea hand: Design, modeling, and sensor processing," *IEEE J. Ocean. Eng.*, vol. 24, no. 1, pp. 96–111, Jan. 1999.

[31] M. Cianchetti, A. Arienti, M. Follador, B. Mazzolai, P. Dario, and C. Laschi, "Design concept and validation of a robotic arm inspired by the octopus," *Mater. Sci. Eng.: C*, vol. 31, no. 6, pp. 1230–1239, 2011.

[32] K. C. Galloway *et al.*, "Soft robotic grippers for biological sampling on deep reefs," *Soft Robot.*, vol. 3, no. 1, pp. 23–33, 2016.

[33] L. U. Odhner, R. R. Ma, and A. M. Dollar, "Precision grasping and manipulation of small objects from flat surfaces using underactuated fingers," in *Proc. IEEE Int. Conf. Robot. Automat.*, 2012, pp. 2830–2835.

[34] F. Tramacere, L. Beccai, E. Sinibaldi, C. Laschi, and B. Mazzolai, "Adhesion mechanisms inspired by octopus suckers," *Procedia Comput. Sci.*, vol. 7, pp. 192–193, 2011.

[35] K. H. Jeong, "Pressure switch for dust sensor and vacuum cleaner having the same," U.S. Patent 9 661 970, May 30, 2017.

[36] G. J. Monkman, S. Hesse, R. Steinmann, and H. Schunk, "Astrictive prehension," in *Robot Grippers*. New York, NY, USA: Wiley, 2007, ch. 5, pp. 169–225.

[37] S. Wachsmann, "Deep-submergence archaeology," in *The Oxford Handbook of Maritime Archaeology*. Oxford, U.K.: Oxford Univ. Press, 2011, ch. 9, pp. 202–231.

[38] S. F. Hoerner, *Fluid-Dynamic Drag; Practical Information on Aerodynamic Drag and Hydrodynamic Resistance*. Bakersfield, CA, USA: Hoerner Fluid Dynamics, 1965.

[39] D. Tritton, *Physical Fluid Dynamics*. Oxford, U.K.: Oxford Univ. Press, 1988.

[40] T. André, P. Lefèvre, and J.-L. Thonnard, "A continuous measure of fingertip friction during precision grip," *J. Neurosci. Methods*, vol. 179, no. 2, pp. 224–229, 2009.

[41] A. Bicchi, "On the closure properties of robotic grasping," *Int. J. Robot. Res.*, vol. 14, no. 4, pp. 319–334, 1995.

[42] N. C. Dafle *et al.*, "Extrinsic dexterity: In-hand manipulation with external forces," in *Proc. IEEE Int. Conf. Robot. Automat.*, 2014, pp. 1578–1585.


**Hannah S. Stuart** (M'11) received the Bachelor's degree in mechanical engineering from the George Washington University, Washington, DC, USA, in 2011 and the Ph.D. degree in mechanical engineering from Stanford University, Stanford, CA, USA, in 2018.

She is currently an Assistant Professor in mechanical engineering with the University of California, Berkeley, CA, USA, where she founded the Embodied Dexterity Group. Her research interests include hand mechanisms, touch perception, design for autonomous or teleoperated interventions, and bioinspired manipulation strategies.

Dr. Stuart is a member of the American Society of Mechanical Engineers.

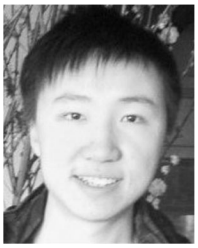

**Shiquan Wang** received the Bachelor's degree in mechatronic engineering from Zhejiang University, Hangzhou, China, in 2012 and the Ph.D. degree in mechanical engineering from Stanford University, Stanford, CA, USA, in 2017.

He is the Founder and CEO of Flexiv Robotics Ltd., Santa Clara, CA. His research interests include human-scale robot locomotion and manipulation, dexterous hand design, contact modeling and dynamic simulation, sensing and actuation system for articulated robots.

Dr. Wang was a recipient of the Best Paper for Safety, Security and Rescue Robotics at the 2016 IEEE/RSJ International Conference on Intelligent Robots and Systems.

**Mark R. Cutkosky** (F'12) received the Ph.D. degree in mechanical engineering from Carnegie Mellon University, Pittsburgh, PA, USA, in 1985.

He is the Fletcher Jones Professor in mechanical engineering with Stanford University, Stanford, CA, USA. His research interests include bioinspired robots, haptics, and rapid prototyping processes.

Dr. Cutkosky is a Fellow of the American Society of Mechanical Engineers.